






# Genetically predicted white matter microstructure mediates the relationship between risk factors and lacunar stroke

Jie Zhang <sup>1,2,3</sup>, Min Wu <sup>2,4</sup>, Douglas Neville,<sup>3</sup> Yue Zou,<sup>5</sup> Kaisi Ren,<sup>1</sup> Qing Ye,<sup>1</sup> Shuchang Zhong,<sup>1</sup> Haiying Xiang,<sup>1</sup> Wenshi Wang,<sup>1</sup> Xiangming Ye <sup>1</sup>, Benyan Luo <sup>2</sup>, Li Zhang <sup>1</sup>

**To cite:** Zhang J, Wu M, Neville D, *et al.* Genetically predicted white matter microstructure mediates the relationship between risk factors and lacunar stroke. *Stroke & Vascular Neurology* 2025;0. doi:10.1136/svn-2025-004208

► Additional supplemental material is published online only. To view, please visit the journal online (<https://doi.org/10.1136/svn-2025-004208>).

Received 5 March 2025  
Accepted 4 June 2025

## ABSTRACT

**Background and purpose** Lacunar stroke is a complex, multifactorial disease with significant genetic underpinnings. However, the mechanisms through which genetic predispositions and risk factors contribute to its pathogenesis remain poorly understood. We investigated whether genetically predicted white matter (WM) microstructure mediates causal relationships between risk factors and lacunar stroke.

**Methods** Data from genome-wide association studies were used to perform two-sample Mendelian randomisation (MR) analyses. Genetic variants associated with risk factors (n=34 461–898 130), lacunar stroke (n=232 596) and eight MRI-derived WM microstructural metrics across 48 tracts (n=20 859–20 860) were analysed. Univariable MR assessed causal effects of risk factors on lacunar stroke. Two-step MR analysis evaluated mediation roles of WM microstructure, whereas multivariable MR accounted for confounders.

**Results** Hypertension was identified as the strongest risk factor for lacunar stroke (OR=1.38; 95% CI: 1.28 to 1.50, p=4.43×10<sup>-15</sup>). Only hypertension showed a significant causal association with genetically predicted WM microstructure. Elevated mean diffusivity (MD), isotropic volume fraction (ISOVF) and the tertiary eigenvalue in the anterior limb of the internal capsule (ALIC) were independently linked to increased lacunar stroke risk, beyond the influence of WM hyperintensities, dilated perivascular spaces and brain volume. Mediation analysis suggested that hypertension-induced lacunar stroke was partially mediated through bilateral MD and left ISOVF in the ALIC, with mediation proportions of 23.70%–33.44%.

**Conclusions** Hypertension may contribute to lacunar stroke pathogenesis in part through WM microstructure alterations, particularly in the ALIC. MD and ISOVF in the ALIC may serve as structural brain reserves and early biomarkers of hypertension-induced pathophysiology associated with lacunar stroke.

## INTRODUCTION

Lacunar stroke is a subtype of stroke characterised by small subcortical infarcts resulting from the blockage of a single penetrating cerebral artery branch. It accounts for 15%–26% of all ischaemic strokes, leading to clinical lacunar syndromes.<sup>1</sup> Primarily attributed to cerebral small vessel disease (CSVD),

## WHAT IS ALREADY KNOWN ON THIS TOPIC

⇒ Lacunar stroke, a subtype of stroke caused by small subcortical infarcts, has strong genetic and vascular risk factors, particularly hypertension and diabetes. While white matter (WM) abnormalities are associated with both lacunar stroke and its risk factors, their role in mediating this relationship remains unclear. Prior genetic studies have established the heritability of lacunar stroke but have largely overlooked WM microstructure as a potential mechanistic link.

## WHAT THIS STUDY ADDS

⇒ Using two-sample Mendelian randomisation (MR) and two-step MR mediation analysis, this study demonstrates that genetically predicted alterations in WM microstructure, particularly in the anterior limb of the internal capsule, partially mediate the causal pathway from hypertension to lacunar stroke. Mean diffusivity and isotropic volume fraction emerge as key mediators, independent of other neuroradiographic features, advancing our understanding of the microstructural mechanisms underlying lacunar stroke risk.

## HOW THIS STUDY MIGHT AFFECT RESEARCH, PRACTICE OR POLICY

⇒ These findings highlight WM integrity as a potential biomarker for early intervention in hypertensive individuals at risk of lacunar stroke. By identifying specific WM microstructural markers as early indicators of lacunar stroke susceptibility, this study supports precision medicine approaches in stroke prevention and underscores the need for strategies aimed at preserving WM health to mitigate lacunar stroke risk.



© Author(s) (or their employer(s)) 2025. Re-use permitted under CC BY-NC. No commercial re-use. See rights and permissions. Published by BMJ Group.

For numbered affiliations see end of article.

## Correspondence to

Dr Benyan Luo;  
luobenyan@zju.edu.cn

Dr Li Zhang;  
zhangli0407@zju.edu.cn

its pathophysiology involves endothelial dysfunction and blood–brain barrier (BBB) disruption, leading to microvascular damage.<sup>2</sup> However, uncertainties surrounding its aetiology hinder the development of effective prevention and treatment strategies.

Hypertension is recognised as the main risk factor for lacunar stroke,<sup>2</sup> alongside smoking, ageing and diabetes.<sup>3</sup> Pooled patient analyses and genome-wide association studies (GWASs) suggest causal links between these factors and

lacunar stroke.<sup>4</sup> Despite its multifactorial nature, interindividual variability in susceptibility to risk factors suggests a genetic basis. For instance, family history of stroke has been associated with sporadic lacunar stroke, and GWASs reveal a significant heritability of MRI-confirmed lacunar stroke.<sup>5</sup> Meta-analysis of GWAS data has identified genetic loci associated with lacunar stroke, highlighting the role of neural substrates as mediators bridging risk factors and lacunar stroke.<sup>4</sup>

MRI advances have increased sensitivity for small infarcts of lacunar stroke, revealing their preferential localisation around white matter (WM) hyperintensities (WMHs).<sup>6</sup> This aligns with GWAS results, which identified shared genetic loci linked to both lacunar stroke and WMHs.<sup>4</sup> Although WMHs serve as an *in vivo* surrogate for underlying pathology, advanced imaging, including diffusion tensor imaging (DTI) and neurite orientation dispersion and density imaging (NODDI), reveals microstructural variability before overt abnormalities develop. DTI captures the impact of genetic loci on CSVD-related traits beyond WMHs.<sup>7</sup> NODDI further enhances biological interpretation.<sup>8</sup> Additionally, WM is particularly susceptible to vascular risk factors like hypertension<sup>9 10</sup> and diabetes.<sup>11</sup> Chronic vascular changes are strongly associated with myelin and axon degeneration, underscoring the interplay between these factors. Given WM's dual association with lacunar stroke and risk factors, we hypothesise WM microstructure may mediate their relationship.

Traditional cohort studies face limitations, including confounding factors and long-term follow-up requirements. Mendelian randomisation (MR) uses genetic instruments to infer causal relationships, reducing bias and reverse causality. Although previous MR studies have linked risk factors to lacunar stroke<sup>4</sup> and CSVD markers,<sup>12</sup> they have not explored mediation pathways. Furthermore, several GWAS and MR studies using imaging-derived phenotypes (IDPs) rely on global metrics,<sup>12 13</sup> overlooking the variability across tracts. This limits insights into tract-specific vulnerabilities critical to lacunar stroke pathogenesis. Additionally, as key markers of CSVD, WMHs reflect demyelination and axonal loss owing to chronic ischaemia,<sup>14</sup> whereas enlarged perivascular spaces (PVSS) indicate impaired interstitial fluid clearance.<sup>15</sup> However, previous genetic studies on WM neglected their impact.

To address these gaps, this study aimed to (1) assess whether genetically predicted WM microstructure mediates the relationship between risk factors and lacunar stroke, (2) explore spatial variability across tracts and (3) determine whether WM microstructure is independent of neuroradiographic confounders.

## METHODS

### Study design

This study used a two-sample MR design, employing genetic instrumental variables (IVs) derived from summary-level GWAS datasets from various consortia

and cohorts. First, a two-sample MR was performed to evaluate the causal effect of risk factors on the incidence of lacunar stroke. Next, multivariable MR was applied to assess whether the impact of WM microstructure on lacunar stroke risk was independent of other imaging markers associated with CSVD. Finally, a two-step MR mediation analysis was conducted to investigate whether WM microstructure mediated the relationship between risk factors and lacunar stroke. This was achieved by evaluating 1) the effect of risk factors on WM microstructure and (2) the impact of WM microstructure on lacunar stroke (figure 1).

### Data sources

Summary-level statistics for exposures, outcomes, mediators and covariates were obtained from GWAS data (table 1). To reduce heritable confounding, data on exposures, mediators and covariates were restricted to individuals of European ancestry, with 97% of the outcome data also derived from European populations.

### Exposures

Exposure traits were categorised based on the established lacunar stroke risk factors<sup>3 4</sup>: (1) dichotomous variables (hypertension, type 2 diabetes, hyperlipidaemia and lipoprotein metabolism disorders) and (2) continuous variables (cigarette smoking, homocysteine levels, body mass index, telomere length and intrinsic epigenetic age acceleration). GWAS data for hypertension (n=412 113), hyperlipidaemia (n=365 889), lipoprotein metabolism disorders (n=395 429) and body mass index (n=290 820) were obtained from FinnGen.<sup>16</sup> GWAS summary data for type 2 diabetes (n=898 130)<sup>17</sup> and homocysteine levels (n=44 147)<sup>18</sup> were obtained from meta-analyses. Lifestyle factors were derived from the GWAS and Sequencing Consortium of Alcohol and Nicotine use, with cigarette use measured as cigarettes per day (n=337 334).<sup>19</sup> In addition, as ageing is a strong risk factor for lacunar stroke, we included genetic proxies for biological ageing: genetically predicted leucocyte telomere length was obtained from UK Biobank data (n=472 174),<sup>20</sup> while intrinsic epigenetic age acceleration, reflecting the deviation of DNA methylation-predicted age from chronological age, was obtained from meta-analyses (n=34 461).<sup>21</sup>

### Outcomes

The primary outcome was lacunar stroke, with GWAS data obtained from a meta-analysis (n=232 596).<sup>22</sup> Diagnosis was made following the Trial of ORG 10172 in Acute Stroke Treatment criteria, requiring both clinical lacunar syndrome and the absence of non-lacunar stroke aetiologies, confirmed via CT.<sup>23</sup> For patients with MRI-verified lacunar stroke, the radiological criteria were as follows: (1) a subcortical infarct of <15 mm, consistent with the clinical syndrome; (2) high-intensity lesions on diffusion-weighted imaging for acute infarcts or (3) low-intensity lesions on T1-weighted or fluid-attenuated inversion recovery imaging for nonacute infarcts.<sup>24</sup>

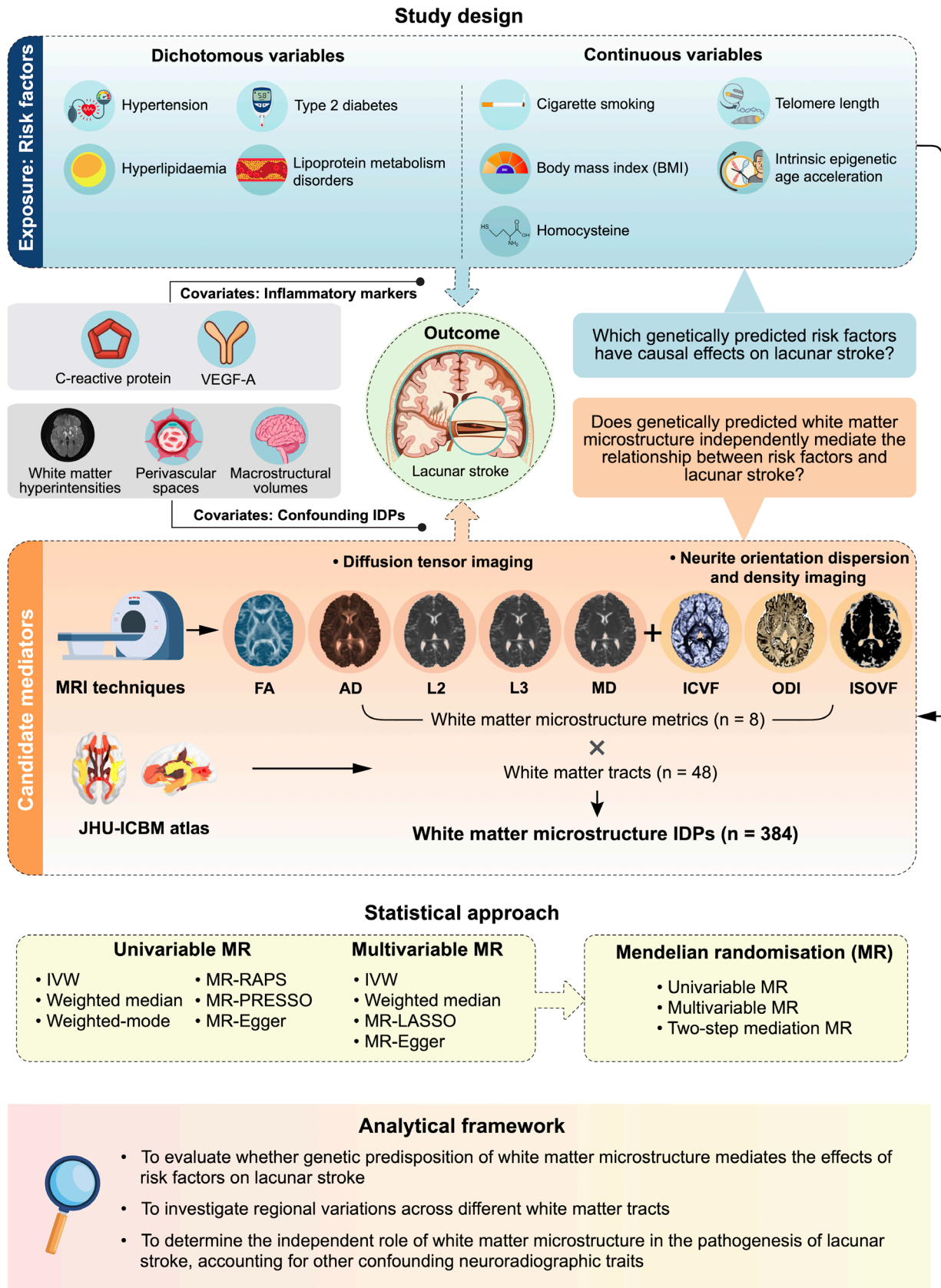


**Figure 1** Overview of the study design. AD, axial diffusivity; FA, fractional anisotropy; ICVF, intracellular volume fraction; IDPs, imaging-derived phenotypes; ISOVF, isotropic volume fraction; IVW, inverse variance-weighted; JHU-ICBM, Johns Hopkins University International Consortium for Brain Mapping; MD, mean diffusivity; MR, Mendelian randomisation; MR-PRESSO, MR pleiotropy residual sum and outlier; MR-RAPS, MR robust adjusted profile score; ODI, Orientation Dispersion Index; VEGF-A, vascular endothelial growth factor A.

**Table 1** Overview of the GWAS data sources used in the study

Phenotype	Unit	Sample size (case/control)	Ancestry	Consortium/ cohort	Year of release/ publication	PubMed ID
Exposure: risk factors						
Dichotomous variables						
Hypertension	Event	122 996/289 117	European	FinnGen	2023	36653562
Lipoprotein metabolism disorders	Event	43 197/352 232	European	FinnGen	2023	36653562
Hyperlipidaemia	Event	13 657/352 232	European	FinnGen	2023	36653562
Type 2 diabetes	Event	74 124/824 006	European	Meta-analysis	2018	30297969
Continuous variables						
Cigarette smoking (cigarettes per day)	SD	337 334	European	GSCAN	2019	30643251
Hyperhomocysteinaemia	SD	44 147	European	Meta-analysis	2013	23824729
Body mass index	SD	290 820	European	FinnGen	2023	36653562
Telomere length	SD	472 174	European	UK Biobank	2021	34611362
Intrinsic epigenetic age acceleration	SD	34 461	European	Meta-analysis	2021	34187551
Outcome: disease						
Lacunar stroke	Event	7338/225 258	Mixed (97% European)	Meta-analysis	2021	33773637
Mediator: white matter microstructure						
Five DTI metrics for 48 tracts*	SD	20 860	European	UK Biobank	2021	33875891
Three NODDI metrics for 48 tracts†	SD	20 859	European	UK Biobank	2021	33875891
Covariate: inflammatory biomarkers						
C reactive protein	SD	575 531	European	Meta-analysis	2022	39794498
Vascular endothelial growth factor A	SD	73 608	European	Meta-analysis	2025	35459240
Covariate: confounding radiological traits						
Brain volume (normalised)	SD	22 138	European	UK Biobank	2021	33875891
White matter volume (normalised)	SD	22 138	European	UK Biobank	2021	33875891
White matter hyperintensities volume	SD	21 381	European	UK Biobank	2021	33875891
Enlarged perivascular space						
White matter	SD	38 598	European	Meta-analysis	2023	37069360
Basal ganglia	SD	38 903	European	Meta-analysis	2023	37069360
Hippocampus	SD	38 871	European	Meta-analysis	2023	37069360

\*The five DTI metrics include fractional anisotropy, mean diffusivity, axial diffusivity and the secondary and tertiary eigenvalues. The 48 tracts are based on the Johns Hopkins University International Consortium for Brain Mapping (JHU-ICBM) atlas.

†The three NODDI metrics include the intracellular volume fraction, isotropic volume fraction and orientation dispersion index. The 48 tracts are based on the JHU-ICBM atlas.

DTI, diffusion tensor imaging; GSCAN, Genome-Wide Association Studies & Sequencing Consortium of Alcohol & Nicotine use; GWAS, genome-wide association studies; NODDI, neurite orientation dispersion and density imaging.

## Mediators

The mediator of interest, WM microstructure, was assessed using the diffusion MRI data from the UK Biobank.<sup>25</sup> Eight diffusion metrics were selected: fractional anisotropy (FA), mean diffusivity (MD), axial diffusivity (AD), and the secondary (L2) and tertiary (L3) eigenvalues, representing diffusion along the radial axes derived from DTI (n=20 860), and intracellular volume fraction (ICVF), isotropic volume fraction (ISOVF), and Orientation Dispersion Index (ODI) from NODDI (n=20 859). A total of 384 IDPs from 48 WM tracts, based on the Johns

Hopkins University International Consortium for Brain Mapping (JHU-ICBM) atlas, were included as potential mediators.

## Covariates

To account for confounding in the relationship between WM microstructure and lacunar stroke, we included other CSVD markers as covariates, such as WMHs and dilated PVS. WMH volume data were obtained from the UK Biobank (n=21 381) using the Brain Intensity AbNormality Classification Algorithm.<sup>25</sup> The GWAS data

on PVS burden were obtained from a series of meta-analyses on WM (n=38 598), basal ganglia (n=38 903) and hippocampus (n=38 871).<sup>26</sup> Normalised whole brain volume (n=22 138) and WM volume (n=22 138) were included as covariates to control for inter-individual macrostructural variability.<sup>25</sup> To mitigate potential bias from unbalanced horizontal pleiotropy and genetic heterogeneity, particularly relevant for risk factors such as hypertension, we additionally adjusted for genetically predicted systemic inflammatory markers, including C reactive protein (CRP) (n=5 75 531)<sup>27</sup> and vascular endothelial growth factor A (VEGF-A) from meta-analyses (n=73 608).<sup>28</sup>

### Sample overlap

We examined the potential for sample overlap between exposure GWAS and the lacunar stroke GWAS. Overlap possibility was estimated based on cohort sources. The bias and type 1 error rate for sample overlap were assessed using an online calculator (<https://sb452.shinyapps.io/overlap/>).<sup>29</sup>

### Genetic instrument and validation

Single-nucleotide polymorphisms (SNPs) with significant genome-wide associations ( $p < 5 \times 10^{-8}$ ) were selected as genetic instruments. Clumping was performed using PLINK to ensure linkage disequilibrium (LD) independence (LD  $r^2 < 0.001$  within a 10 000 kb window). When exposure SNPs were missing from the outcome GWAS data, proxy SNPs with high LD ( $r^2 > 0.8$ ) were identified using LDlink. Data harmonisation was conducted to align allele orientation across datasets (online supplemental table S1). Instrument strength and statistical power were evaluated (see details in online supplemental eMethods).

### Statistical analysis

#### Univariable MR analysis

Univariable MR analyses were conducted to assess the causal relationships between (1) risk factors and lacunar stroke, (2) WM microstructural IDPs and lacunar stroke and (3) risk factors and WM microstructural IDPs. The primary analysis used the random-effects inverse-variance weighted (IVW) method to combine individual Wald ratio estimates into a pooled effect. MR Steiger tests were used to determine the directionality of causal pathways and identify potential reverse causality. Additionally, a bidirectional MR was performed to further evaluate the causal relationship between WM microstructure and lacunar stroke; in the reverse analysis, genetic liability for lacunar stroke was considered as the exposure.

Effect sizes were reported as ORs for lacunar stroke per one SD increase in risk factors or IDPs. When IDPs were used as outcomes, effect sizes ( $\beta$ ) represented the changes in WM microstructure with each SD increase in risk factors. For spatial mapping, the association between WM tracts and IDPs was visualised using the JHU-ICBM atlas for regional interpretation. Bonferroni correction

was applied to account for multiple comparisons (see details in online supplemental eMethods).

#### Multivariable MR analysis

Significant associations identified in the univariable MR were further evaluated using multivariable MR. This approach accounted for the influence of additional covariates, including WMHs, PVS burden, whole brain volume and WM volume. Genetic instruments for different IDPs were clumped to ensure independence (LD  $r^2 < 0.001$ , window=10 000 kb). The multivariable IVW method was applied to quantify the independent effect of each risk factor.

#### MR mediation analysis

A two-step MR mediation analysis was performed to explore whether WM microstructural metrics mediated the effect of risk factors on lacunar stroke.<sup>30</sup> In the first step, genetic instruments for risk factors that showed a significant total effect on lacunar stroke ( $\beta_{\text{total}}$ ) were used to assess the effect of each risk factor on WM microstructure ( $\beta_1$ ). The second step involved the assessment of the effect of WM microstructure on lacunar stroke ( $\beta_2$ ). The indirect effect was calculated using the product of coefficients method. SEs for indirect effects were calculated using the delta method. In the multivariable MR analysis assessing independent effects, we adjusted for relevant neuroradiographic covariates (as detailed above) to isolate regional microstructural contributions. However, to avoid overadjustment in the mediation estimates, these covariates were not included in the subsequent two-step mediation analyses.

To ensure the validity of causal inference and the temporal sequence required in the mediation framework, we leveraged inherent features of the MR design and reiterated key directionality checks. First, the use of germline genetic variants, fixed at conception, ensures the assumption that exposures temporally precede downstream mediators and outcomes. Second, as detailed above, we applied three strategies to reinforce this assumption, summarised as follows: (1) Instrument selection: all SNPs were selected based on genome-wide significance ( $p < 5 \times 10^{-8}$ ); (2) MR-Steiger tests: these were used to statistically verify the direction of effect across each causal step (risk factor to WM microstructure, risk factor to lacunar stroke, and WM microstructure to lacunar stroke) and (3) Bidirectional MR: reverse-direction analyses were performed to explicitly rule out reverse causality. Collectively, these strategies jointly confirmed the temporal plausibility and causal directionality underlying the hypothesised mediation model.

#### MR sensitivity analysis

Given that the IVW method assumes valid IVs across all genetic variants, sensitivity analyses were conducted to assess the robustness of the findings. These analyses addressed potential violations of MR assumptions, including horizontal pleiotropy and weak instruments,

by employing various methods: (1) the weighted median method provides consistent estimates even if up to 50% of the variants are invalid instruments due to horizontal pleiotropy; (2) the weighted mode method clusters variants based on similarity in causal effects and derives estimates from the largest SNP cluster; (3) MR-Egger regression identifies directional pleiotropy using an intercept term and adjusts the estimates accordingly; (4) MR-robust adjusted profile score (MR-RAPS) corrects for weak instruments by accounting for variability in instrument strength; (5) MR Pleiotropy RESidual Sum and Outlier (MR-PRESSO) detects and removes influential outliers to reassess results without bias and (6) MR least absolute shrinkage and selection operator (MR-LASSO) mitigates multicollinearity among IVs by penalising less relevant SNPs.

In the univariable MR analysis, estimates were calculated using the weighted median, weighted mode, MR-Egger, MR-RAPS and MR-PRESSO methods. Cochran's Q statistic was used to assess heterogeneity across SNP-specific causal estimates, and funnel plots were created to evaluate the balance of pleiotropic effects among the instruments. Additionally, leave-one-SNP-out analyses were performed to identify individual SNPs with excessive influence on the pooled effects. For the multivariable MR analysis, the multivariable extensions of the weighted median, MR-Egger and MR-LASSO methods were used to assess the robustness of causal estimates under multivariable conditions.

All analyses were performed using R software (V.4.3.2; the R Foundation for Statistical Computing, Vienna, Austria). The TwoSampleMR (V.0.10.0), mr.raps (V.0.2) and MRPRESSO (V.1.0) packages were used for conducting all univariable MR analyses, whereas the MendelianRandomization (V.0.5.1) and MVMR (V.0.4) packages were used for conducting multivariable MR analyses. The R code supporting all MR analyses in this study can be found on GitHub: [https://github.com/jzhang-neuro/MR\\_WM\\_LS](https://github.com/jzhang-neuro/MR_WM_LS).<sup>31</sup>

## RESULTS

### General framework of the MR study

The MR analysis framework is illustrated in figure 1. Nine risk factors were selected as exposure variables, 384 WM microstructural IDPs as candidate mediators and 6 confounding radiological features and two inflammatory biomarkers as covariates, with lacunar stroke designated as the outcome. Detailed variable characteristics based on the GWAS dataset are presented in table 1.

### Total effect of risk factors on lacunar stroke

Univariable MR analysis using the IVW method identified a genetic predisposition to hypertension as the strongest risk factor for lacunar stroke incidence (OR=1.38; 95% CI: 1.28 to 1.50,  $p=4.43 \times 10^{-15}$ ), with consistent results across multiple pleiotropy-robust methods including weighted median, MR-RAPS and MR-PRESSO (figure 2).

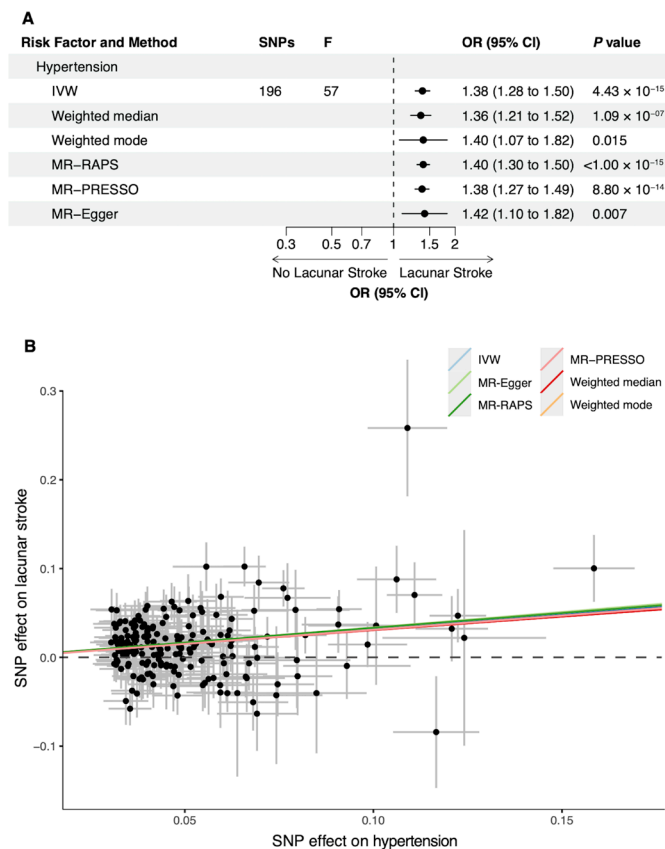


**Figure 2** Univariable MR estimates of the causal relationships between hypertension and lacunar stroke. (A) Forest plot shows the main causal effect estimates derived from IVW and the sensitivity analyses using different methods. (B) Scatter plot of SNP effects on hypertension versus lacunar stroke, with the slope of each line corresponding to the estimated MR effect per method. IVW, inverse variance-weighted; MR, Mendelian randomisation; MR-PRESSO, MR pleiotropy residual sum and outlier; MR-RAPS, MR robust adjusted profile score; SNPs, single-nucleotide polymorphisms.

Additionally, type 2 diabetes (OR=1.13; 95% CI: 1.07 to 1.19,  $p=5.27 \times 10^{-6}$ ) and lipoprotein metabolism disorders (OR=1.18; 95% CI: 1.07 to 1.31,  $p=0.0009$ ) were significantly associated with an elevated risk of lacunar stroke (online supplemental figure S1). Other risk factors were not significantly associated. To address the potential inflation of causal estimates due to high collinearity between hyperlipidaemia and lipoprotein metabolism disorders, we conducted a multivariable MR analysis including both traits as exposures and lacunar stroke as the outcome. After mutual adjustment, neither lipoprotein metabolism disorders (IVW OR=0.99, 95% CI: 0.48 to 2.05,  $p=0.98$ ) nor hyperlipidaemia (IVW OR=1.19, 95% CI: 0.58 to 2.45,  $p=0.63$ ) remained significantly associated (online supplemental figure S2). However, conditional F-statistics were below the conventional threshold ( $F < 1$ ), indicating weak instrument bias and high collinearity, which may have limited the power to detect independent effects.

Sensitivity analyses confirmed the robustness of the associations between all the risk factors and lacunar stroke,

with no evidence of pleiotropy (online supplemental table S2). Cochran's  $Q$  test identified IV heterogeneity for hypertension ( $Q=270.60$ ,  $p=0.0002$ ; online supplemental table S3), although the IV strength remained adequate ( $F\geq 39$ ). In addition, we conducted multivariable MR analyses adjusting for inflammatory biomarkers, including CRP and VEGF-A, to evaluate potential residual pleiotropy through inflammation-related pathways. The causal effect of genetically predicted hypertension on lacunar stroke remained significant after adjustment for CRP (IVW OR=1.31; 95% CI: 1.19 to 1.43;  $p=9.76\times 10^{-9}$ ) and VEGF-A (IVW OR=1.40; 95% CI: 1.29 to 1.52;  $p=1.06\times 10^{-15}$ ), with consistent results observed across weighted median, MR-Egger and MR-LASSO methods (online supplemental figure S3). These findings mitigate concerns about unbalanced pleiotropy driven by inflammation. MR Steiger analysis ruled out reverse causality (online supplemental table S4), and leave-one-SNP-out plots showed no single influential variant (online supplemental figures S4–S6), and the funnel plot did not indicate potential biases or pleiotropy (online supplemental figure S7).

Based on cohort sources, we expect no substantial sample overlap for most exposures (online supplemental table S5). Minimal overlap may exist for cigarette smoking and telomere length, but the potential bias is considered negligible. Across assumed sample overlap rates of 10%, 50% and 90%, the estimated bias remained extremely small (range: 0.000–0.007), and the type 1 error rate was consistently around 0.05 (online supplemental table S5). These findings suggest that any potential sample overlap would not materially bias our MR results.

### Effect of hypertension on WM microstructure

IVW analyses showed hypertension was associated with increased L2, L3, MD and ISOVF in multiple WM tracts, including the bilateral anterior limb of the internal capsule (ALIC), retrolenticular portion of the internal capsule, anterior corona radiata and external capsule (figure 3A). Detailed summaries of the causal effects of greater hypertension risk on the genetic predisposition to lower FA and higher MD, ISOVF and eigenvalues across all significant tracts are provided in online supplemental tables S6 and S7. By contrast, type 2 diabetes and lipoprotein metabolism disorders showed no significant tract-specific relationships (online supplemental figures S8 and S9 and online supplemental tables S8–S11). MR-Egger test for pleiotropy (online supplemental tables S12–S14), Cochran's  $Q$  heterogeneity test (online supplemental tables S15–S17) and Steiger test for directionality (online supplemental tables S18–S20) are summarised in the online supplemental material.

### Effect of WM microstructure on lacunar stroke

The associations between WM microstructure and lacunar stroke identified in the univariable MR analyses are detailed in online supplemental tables S21 and S22. Figure 3B spatially visualises the distribution of significant

results along the WM tracts. IVW analyses demonstrated that every genetically predicted 1-SD increase in MD and L3 in the left ALIC (MD: OR=1.95; 95% CI: 1.43 to 2.66,  $p=2.33\times 10^{-5}$ ; L3: OR=1.91; 95% CI: 1.45 to 2.51,  $p=4.20\times 10^{-6}$ ), right ALIC (MD: OR=2.03; 95% CI: 1.45 to 2.85,  $p=3.50\times 10^{-5}$ ; L3: OR=2.00; 95% CI: 1.57 to 2.55,  $p=1.74\times 10^{-8}$ ) and ISOVF in the right ALIC (OR=2.72; 95% CI: 1.62 to 4.56,  $p=1.49\times 10^{-4}$ ) significantly increased lacunar stroke risk (figure 4). These associations remained significant after sensitivity, analyses with heterogeneity noted in bilateral ALIC MD (online supplemental table S23), but no evidence of pleiotropy (online supplemental table S24) or reverse causality (online supplemental tables S25 and S26).

### Independent effect of WM microstructure on lacunar stroke

Multivariable MR analyses, adjusted for WMH volume, confirmed that higher MD and L3 in the left ALIC (MD: OR=1.90; 95% CI: 1.44 to 2.50,  $p=4.74\times 10^{-6}$ ; L3: OR=2.09; 95% CI: 1.59 to 2.76,  $p=1.71\times 10^{-7}$ ), right ALIC (MD: OR=1.91; 95% CI: 1.39 to 2.62,  $p=7.07\times 10^{-5}$ ; L3: OR=2.03; 95% CI: 1.56 to 2.63,  $p=9.28\times 10^{-8}$ ) and higher ISOVF in the right ALIC (OR=2.41; 95% CI: 1.79 to 3.26,  $p=1.03\times 10^{-8}$ ) were independently associated with increased lacunar stroke risk (online supplemental figure S10). After adjusting for PVS enlargement, the effects of microstructure in the left ALIC (MD: OR=1.46; 95% CI: 1.11 to 1.93,  $p=0.007$ ; L3: OR=1.52; 95% CI: 1.17 to 1.97,  $p=0.002$ ) and right ALIC (MD: OR=1.56; 95% CI: 1.15 to 2.12,  $p=0.004$ ; L3: OR=1.65; 95% CI: 1.30 to 2.11,  $p=4.55\times 10^{-5}$ ; ISOVF: OR=1.98; 95% CI: 1.24 to 3.17,  $p=0.004$ ) on lacunar stroke remained significant. Similarly, after adjusting for whole brain and WM volumes, the associations remained robust, with effect estimates highly consistent with univariable MR. Multivariable MR-Egger intercept analysis did not detect horizontal pleiotropy (online supplemental table S27). Additionally, MR-LASSO confirmed no problematic multicollinearity among the covariates and WM microstructural parameters (online supplemental figure S10). Heterogeneity test statistics are provided in online supplemental table S28.

### Mediation effect of WM microstructure

Two-step MR mediation analysis identified significant mediation effects of WM tract microstructural metrics in the relationship between hypertension and lacunar stroke (figure 5). MD in the left (IVW  $\beta=0.09$ ; 95% CI: 0.04 to 0.13,  $p=3.86\times 10^{-4}$ ) and right ALIC (IVW  $\beta=0.08$ ; 95% CI: 0.03 to 0.13,  $p=0.001$ ), L3 in the left (IVW  $\beta=0.08$ ; 95% CI: 0.04 to 0.12,  $p=3.04\times 10^{-4}$ ) and right ALIC (IVW  $\beta=0.08$ ; 95% CI: 0.04 to 0.12,  $p=1.10\times 10^{-4}$ ) and ISOVF in the right ALIC (IVW  $\beta=0.11$ ; 95% CI: 0.04 to 0.17,  $p=0.001$ ) significantly mediated the effect of hypertension, accounting for 23.70%–33.44% of the total mediation effect (figure 5A). These mediation effects of MD and ISOVF remained robust after adjusting for hypertension (figure 5B).

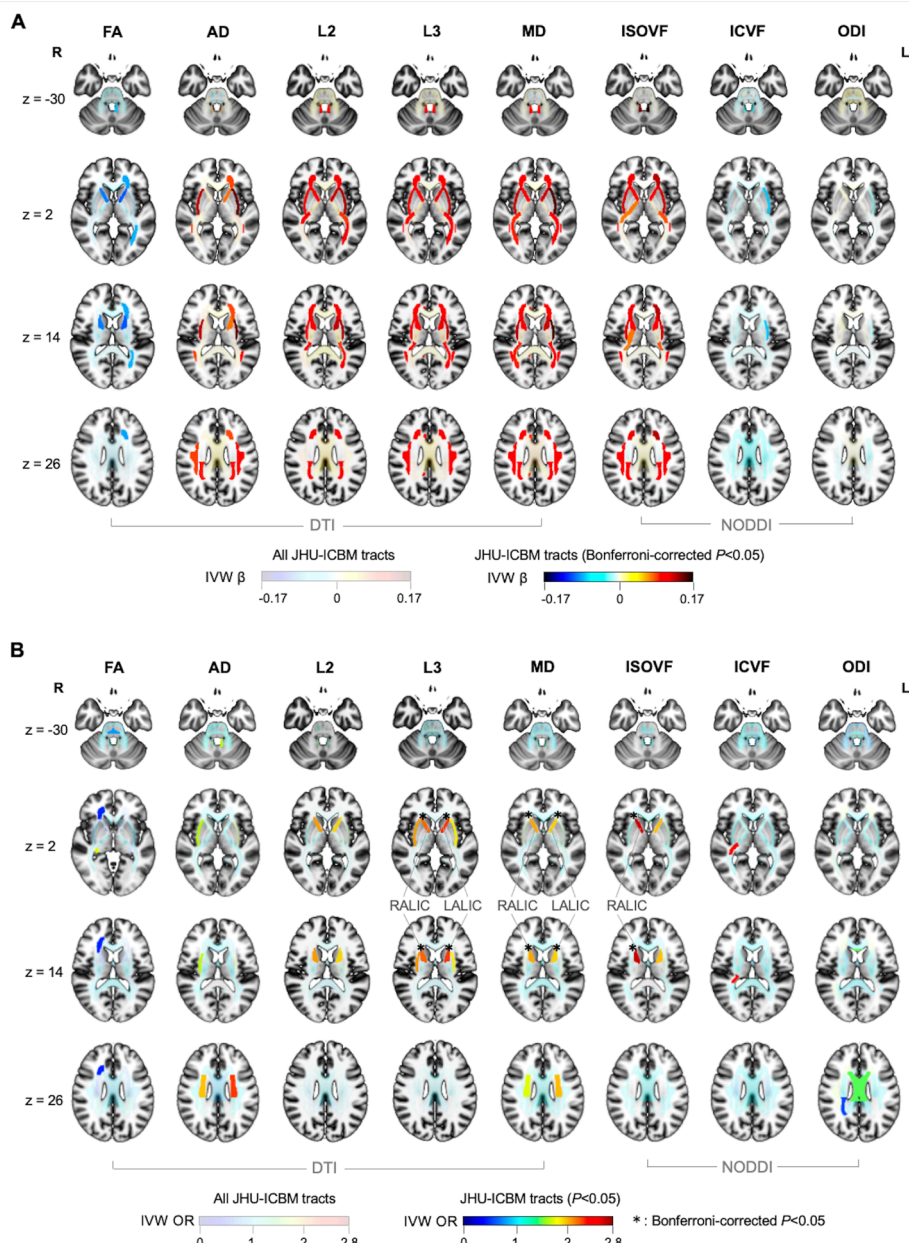


**Figure 3** Effect size mapping of the causal associations with white matter microstructural parameters. (A) Associations between hypertension and white matter microstructural parameters; (B) associations between white matter microstructural parameters and lacunar stroke. The eight columns present the results of the analyses based on the eight microstructural metrics of 48 white matter tracts from the JHU-ICBM atlas. The columns show the results from the five DTI and the three NODDI metrics. The colours of the tracts reflect the IVW  $\beta$  values of the significant associations between hypertension and imaging characteristics after Bonferroni correction. These effect sizes represent the disease risk ORs calculated using the inverse-variance weighted calculation method. AD, axial diffusivity; DTI, diffusion tensor imaging; FA, fractional anisotropy; ICVF, intracellular volume fraction; ISOVF, isotropic volume fraction; IVW, inverse variance-weighted; JHU-ICBM, Johns Hopkins University International Consortium for Brain Mapping; L, left side; MD, mean diffusivity; NODDI, neurite orientation dispersion and density imaging; ODI, Orientation Dispersion Index; R, right side.

## DISCUSSION

This study employed a combination of univariable, multivariable and two-step MR mediation analyses to investigate the causal relationships among risk factors, WM microstructure and lacunar stroke using GWAS data. Hypertension was identified as the strongest causal contributor to lacunar stroke, with its effect partially mediated via the WM microstructure. Specifically, bilateral MD and right

ISOVF in the ALIC were identified as key mediators. Individuals with genetically reduced WM integrity in these regions exhibited greater susceptibility to hypertension-induced lacunar stroke. Because genetically predicted MD and ISOVF represent innate microstructural susceptibility fixed at conception, which precedes both environmental exposures and observable neuroimaging alterations, they allow us to dissect the causal chain from genetic

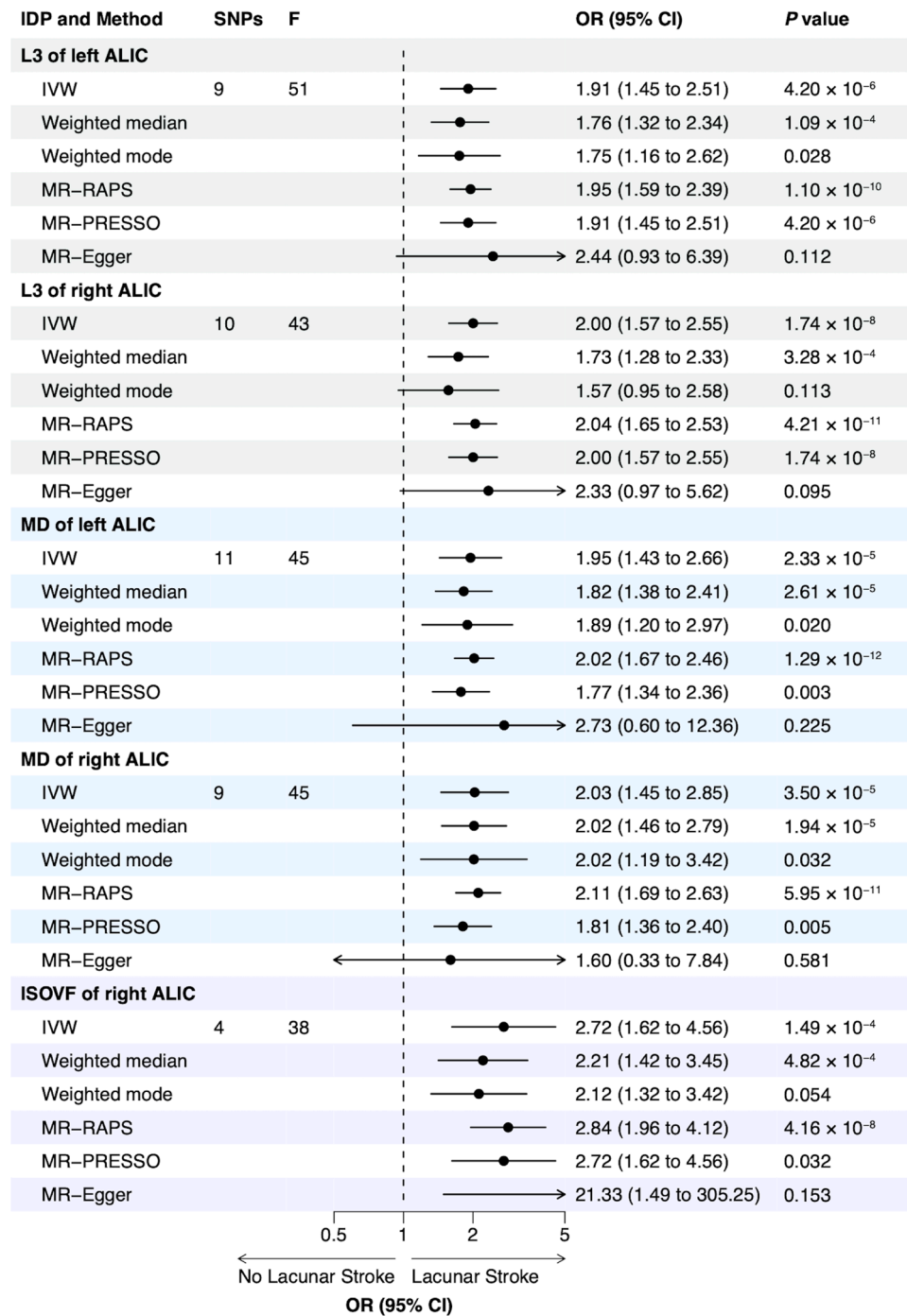


**Figure 4** Univariable MR estimates for the significant causal relationships between white matter microstructure in the ALIC and lacunar stroke. The forest plot shows the primary causal effect estimates derived from IVW and sensitivity analyses using various methods. ALIC, anterior limb of the internal capsule; DTI, diffusion tensor imaging; IDP, imaging-derived phenotype; ISOVF, isotropic volume fraction; IVW, inverse-variance weighted; MD, mean diffusivity; MR, Mendelian randomisation; PRESSO, Pleiotropy RESidual Sum and Outlier; RAPS, Robust Adjusted Profile Score; SNPs, single-nucleotide polymorphisms.

risk to WM microstructural alteration to stroke, rather than merely serving as a contemporaneous indicator of WM condition. This relationship remained stable across sensitivity analyses, even after adjusting for confounders, underscoring the importance of investigating microstructural alterations in the broader context of established pathophysiological mechanisms.

Among the risk factors for lacunar stroke, only hypertension exhibited an indirect effect mediated by the WM microstructure. Previous studies have consistently demonstrated the detrimental effects of hypertension on WM integrity, with microvascular dysfunction driving radiographic WM damage.<sup>32</sup> Biological mechanisms include endothelial dysfunction, reactive gliosis and ischaemic

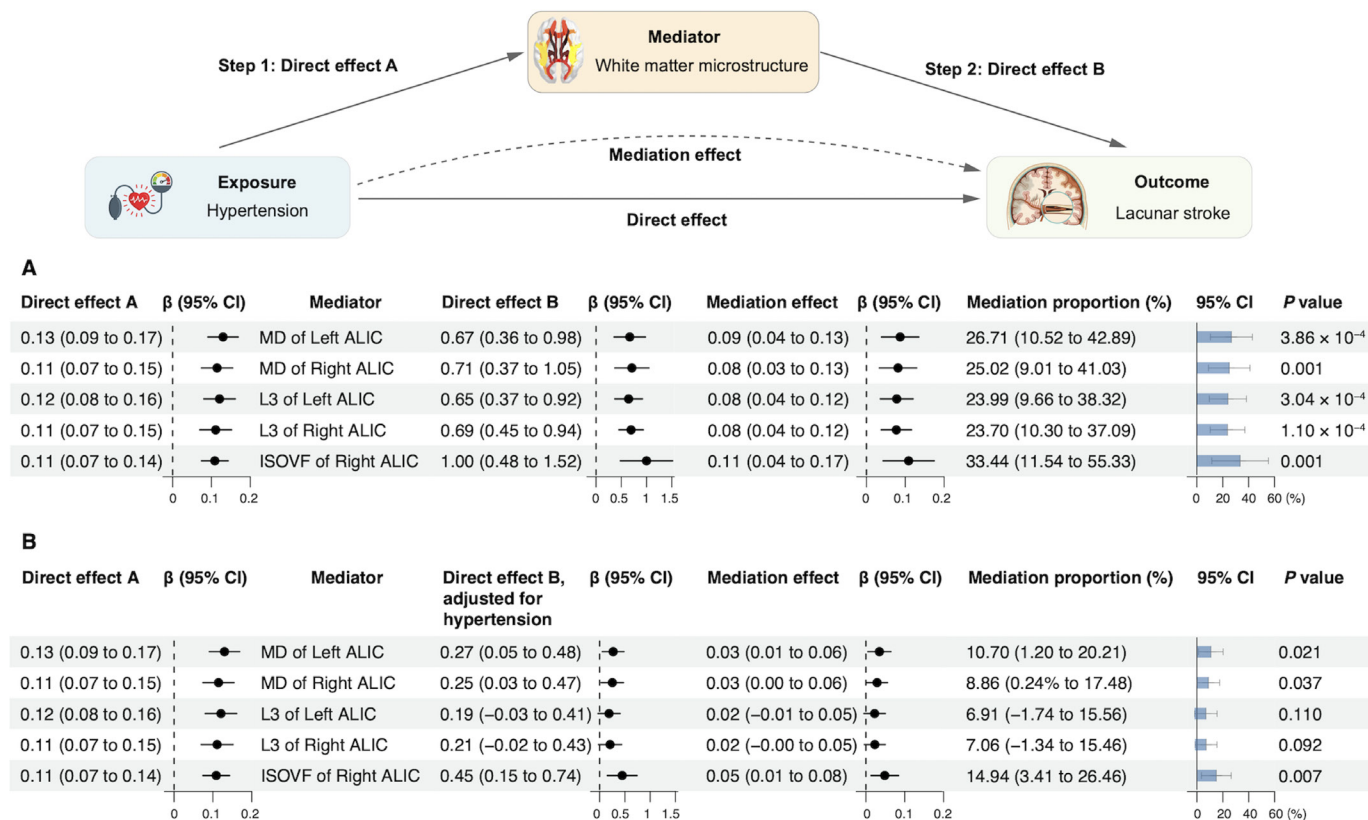


**Figure 5** Mediation effect of hypertension on lacunar stroke via the white matter microstructure in the ALIC. Two-step MR was used to evaluate the mediating role of each white matter microstructure parameter in the causal relationship between hypertension and lacunar stroke. (A) The univariable MR estimates for the causal effects; (B) the multivariable MR estimates for the causal effect of each mediator on lacunar stroke, adjusted for hypertension. ‘Direct effect A’ indicates the effect of hypertension on white matter microstructure, ‘direct effect B’ represents the effect of white matter microstructure on lacunar stroke and ‘mediation effect’ indicates the effect of hypertension on lacunar stroke through the white matter microstructure. All estimates were calculated using the inverse-variance weighted method. ALIC, anterior limb of the internal capsule; ISOVF, isotropic volume fraction; MD, mean diffusivity; MR, Mendelian randomisation.

injury, all of which are exacerbated by chronic hypertension.<sup>33</sup> Furthermore, hypertension disrupts the BBB, triggering neuroinflammation and leading to acute axonal injury and myelin degradation.<sup>34</sup> Hypertension accelerates arteriolosclerosis, impairing the small penetrating arteries that supply subcortical WM, thereby exacerbating WM injury severity.<sup>35</sup> These cumulative changes result in lacune formation,<sup>10</sup> linking microstructural degradation to lacunar stroke.

Given the progressive nature of hypertension-induced WM damage, identifying early microstructural alterations in normal-appearing WM is crucial for achieving timely preventive management. Although demyelination and axonal degeneration are prominent in the chronic stages, acute WM injury typically presents as vasogenic oedema.<sup>10</sup> Increased BBB permeability has been observed in normal-appearing WM in patients with CSVD.<sup>36</sup> In this study, diffusion MRI was used as a non-invasive method for detecting subtle microstructural changes, proving valuable for early diagnosis. Studies demonstrated high blood pressure contributes to WM microstructural decline. Diffusion tractography has shown evidence through altered MD and AD.<sup>9</sup> Furthermore,

associations between higher blood pressure and reduced FA and increased MD in older adults were reported.<sup>37</sup> Other studies have linked higher diastolic blood pressure to reduced FA and ICVF, along with increased MD and ISOVF values.<sup>38</sup> These findings are consistent with our results, underscoring the importance of hypertension management in reducing lacunar stroke risk by preserving WM integrity.

The association between WM microstructure and lacunar stroke has been demonstrated through the correlation of skeletonised MD with CSVD burden, including lacunar infarct count.<sup>39</sup> Additionally, microstructural changes in MD and FA have been observed in WM tracts distant from the primary lacunar infarction site, suggesting widespread structural disruption.<sup>40</sup> However, these studies were limited by their cross-sectional design, lacking evidence on temporal causality. GWASs using LD score regression have also linked global WM metrics with increased lacunar stroke risk.<sup>13</sup> The Steiger test and bidirectional MR showed no reverse causality where lacunar stroke was considered an exposure. Our study advances these findings by providing evidence for specific WM tracts in lacunar stroke pathogenesis.

Among various microstructural parameters, MD and ISOVF emerged as reliable mediators of the hypertension–lacunar stroke relationship. This likely reflects their heightened sensitivity to early microstructural alterations and their ability to capture preclinical pathophysiological changes. MD, which measures the average diffusivity of water molecules within tissues, provides valuable insights into overall WM integrity. Similarly, ISOVF quantifies extracellular fraction of free-water, which tends to increase with neuroinflammation and BBB dysfunction.<sup>8</sup> By contrast, L3, which reflects radial diffusivity and is sensitive to demyelination,<sup>41</sup> showed strong associations with both hypertension and lacunar stroke; however, it no longer maintained its mediating effect after adjusting for hypertension, suggesting its role may be overshadowed by the direct impact of hypertension on WM integrity.

These results suggest that hypertension contributes to lacunar stroke by increasing overall tissue diffusivity, particularly extracellular fluid in WM, rather than altering diffusion directionality, neurite density or fibre dispersion as reflected by FA, ICVF or ODI. Elevated MD and ISOVF can thus serve as early biomarkers of WM injury, detecting hypertension-induced damage before visible WMHs on conventional imaging or changes in other metrics such as FA.<sup>42</sup> Elevated MD and ISOVF values are associated with increased BBB permeability and localised neuroinflammation, aligning with lacunar stroke pathophysiology.<sup>43</sup> Conversely, lower MD and ISOVF values may indicate preserved WM integrity, providing potential neuroprotection against hypertension. Thus, understanding individual WM integrity profiles could enhance personalised strategies for lacunar stroke prevention.

The spatial heterogeneity of WM tracts is also noteworthy. The ALIC, external capsule, superior longitudinal fasciculus and posterior corona radiata have been associated with genetic predispositions to hypertension. Previous DTI research has consistently implicated the ALIC as vulnerable to hypertension-induced diffusion changes.<sup>44</sup> Additionally, a previous study reported that MD alterations occur earlier in anterior than in posterior brain regions.<sup>9</sup> Moreover, a univariate MR study identified significant associations between genetically determined risk of small-vessel stroke and WM microstructure, particularly in the ALIC.<sup>45</sup> Our findings align with these reports, identifying the ALIC as the primary mediator in hypertension-related WM changes. The ALIC, projecting to the prefrontal cortex, supports cognitive functions such as behavioural control.<sup>46</sup> Its susceptibility to vascular damage, particularly within the lenticulostriate arterial territory, may underlie cognitive impairment observed in lacunar stroke.<sup>47</sup> However, the publicly available GWAS data lacks detailed information on the lesion locations of lacunar infarcts, limiting the ability to directly link specific tract changes with the precise location of these infarcts. Future research should investigate the spatial relationships between WM microstructural changes and lacune formation in specific regions, as well as their interaction with established pathophysiological mechanisms.

A key strength of this study is its rigorous consideration of confounding neuroradiographic factors. Previous research has shown that hypertension's effects on WM persist even after accounting for WMH burden.<sup>37–42</sup> Our multivariable MR analysis confirmed these findings and demonstrated that WM microstructure independently mediates lacunar stroke risk, even after accounting for CSVD burden and macrostructural variability. These results underscore the need for early detection and interventions in individuals genetically predisposed to reduced WM integrity.

Despite the strengths of our study, it also has limitations. The accurate selection of genetic instruments and potential pleiotropy could influence causal estimates. However, sensitivity analyses have addressed these concerns, confirming the results' robustness. Second, the available GWAS data on lacunar stroke categorise the outcome as a dichotomous variable, without providing details on the location or extent of lesions. This limitation restricts the ability to differentiate between lesion effects and microstructural changes. However, the lack of significant findings in reverse MR analyses and non-significant Steiger directionality tests support that WM microstructural changes are likely mediating factors in lacunar stroke pathogenesis rather than a consequence. Furthermore, lacunar infarcts may result from heterogeneous mechanisms, including parent artery plaque, microatheroma and lipohyalinosis.<sup>48–50</sup> However, available mechanism-stratified datasets (eg, those for large artery atherosclerosis or small vessel stroke) pertain to general ischaemic stroke and do not specifically capture lacunar stroke aetiologies, thereby limiting the feasibility of subtype-specific MR analyses. As such, our findings may reflect averaged effects across multiple lacunar stroke mechanisms, possibly blunting causal specificity. We, therefore, acknowledge that heterogeneity in underlying mechanisms could introduce noise and bias the effect estimates. Future work incorporating MRI-confirmed subtype classification or mechanism-specific genetic instruments would allow for more refined causal inferences. Additionally, other potential pathways, such as impaired glymphatic clearance, were not explored. Moreover, some confounding factors, like amyloid deposits and microhaemorrhages, were not included owing to limited GWAS data. Future studies incorporating larger GWAS datasets may provide more comprehensive insights. Regarding temporal plausibility, although heterogeneity in the ages and timing of blood-pressure measurements, MRI scans, and stroke assessments across cohorts could theoretically challenge the temporal sequence of 'exposure–mediator–outcome', our MR-Steiger directionality tests and bidirectional MR analyses robustly excluded reverse causality, supporting the temporal plausibility of our mediation framework. Lastly, our analyses were restricted to individuals of European ancestry. While this approach reduces confounding from population stratification, it limits generalisability to other ancestral groups. Given known cross-ancestry differences in the

genetic architecture of lacunar stroke risk factors,<sup>51 52</sup> the magnitude and direction of mediation effects may vary across populations. Future studies incorporating diverse multi-ancestry GWAS datasets will be essential to validate and extend these findings.

## CONCLUSIONS

This study underscores the potential role of genetically predicted WM microstructure as a mediator between hypertension and lacunar stroke. Elevated MD and ISOVF in the ALIC may serve as early biomarkers of hypertension-induced WM injury, potentially increasing susceptibility to lacunar stroke. These findings highlight the need for personalised strategies aimed at preserving WM integrity to reduce the risk of lacunar stroke.

### Author affiliations

<sup>1</sup>Centre for Rehabilitation Medicine, Rehabilitation & Sports Medicine Research Institute of Zhejiang Province, Department of Rehabilitation Medicine, Zhejiang Provincial People's Hospital (Affiliated People's Hospital), Hangzhou Medical College, Hangzhou, Zhejiang, China

<sup>2</sup>Department of Neurology, Brain Medical Centre, The First Affiliated Hospital of Zhejiang University School of Medicine, Hangzhou, Zhejiang, China

<sup>3</sup>Wellcome Centre for Human Neuroimaging, Department of Imaging Neuroscience, Institute of Neurology, University College London, London, UK

<sup>4</sup>Wellcome Centre for Integrative Neuroimaging, FMRIB, Medical Research Council Brain Network Dynamics Unit, Nuffield Department of Clinical Neurosciences, University of Oxford, Oxford, UK

<sup>5</sup>Department for Clinical and Movement Neurosciences, Institute of Neurology, University College London, London, UK

**Contributors** BL and LZ designed the study. JZ, YZ, KR and HX collected the data and performed the data preprocessing. MW, SZ, WW and QY contributed to statistical analysis and data interpretation. XY and DN reviewed the results and verified the conclusions. JZ and MW drafted the manuscript. DN, YZ, KR, QY, SZ, HX, WW, XY, BL and LZ edited the original and revised manuscripts. BL and LZ are the guarantors of this work. All authors confirm that they have full access to all the data in the study and have read and approved the final version of the manuscript.

**Funding** This study was funded by National Natural Science Foundation of China (Grant number: 82272592); Medical Science and Technology Project of Zhejiang Province (Grant numbers: 2024KY771, 2024KY695, 2023KY481, 2021KY457); Key Research and Development Program of Zhejiang Province (Grant number: 2024C03040).

**Competing interests** None declared.

**Patient consent for publication** Not applicable.

**Provenance and peer review** Not commissioned; externally peer reviewed.

**Data availability statement** Data are available in a public, open access repository. All GWAS summary statistics analysed in this study are publicly available. The GWAS data related to risk factor traits were obtained from the FinnGen summary statistics Release 10 for hypertension, lipoprotein metabolism disorders, hyperlipidaemia and body mass index (<https://finngen.gitbook.io/documentation/v/r10/data-download>); GSCAN for cigarette smoking (<https://doi.org/10.1038/s41588-018-0307-5>); meta-analyses for type 2 diabetes (<https://www.ebi.ac.uk/gwas/studies/GCST002087>), hyperhomocysteinaemia (<https://doi.org/10.1038/s41588-018-0241-6>) and intrinsic epigenetic age acceleration (<https://www.ebi.ac.uk/gwas/studies/GCST90014290>); and UK Biobank data were used for leukocyte telomere length (<https://gwas.mrcieu.ac.uk/datasets/ieu-b-4879>). The GWAS data for lacunar stroke were acquired at <https://gwas.mrcieu.ac.uk/datasets/ebi-a-GCST90014123>. GWAS data for WM microstructure, WMHs and macrostructural brain volumes were retrieved from the GWAS Catalog (<https://www.ebi.ac.uk/gwas/publications/33875891>). Summary statistics for PVS burden were retrieved or requested from the authors of the relevant study (<https://doi.org/10.1038/s41591-023-02268-w>). The GWAS data for inflammatory markers were obtained from meta-analyses of CRP (<https://www.ebi.ac.uk/gwas/studies/ebi-a-GCST90029070>) and VEGF-A (<https://www.ebi.ac.uk/gwas/studies/GCST90428438>). The R code

supporting all MR analyses in this study is available on GitHub: [https://github.com/jzhang-neuro/MR\\_WM\\_LS](https://github.com/jzhang-neuro/MR_WM_LS).

**Supplemental material** This content has been supplied by the author(s). It has not been vetted by BMJ Publishing Group Limited (BMJ) and may not have been peer-reviewed. Any opinions or recommendations discussed are solely those of the author(s) and are not endorsed by BMJ. BMJ disclaims all liability and responsibility arising from any reliance placed on the content. Where the content includes any translated material, BMJ does not warrant the accuracy and reliability of the translations (including but not limited to local regulations, clinical guidelines, terminology, drug names and drug dosages), and is not responsible for any error and/or omissions arising from translation and adaptation or otherwise.

**Open access** This is an open access article distributed in accordance with the Creative Commons Attribution Non Commercial (CC BY-NC 4.0) license, which permits others to distribute, remix, adapt, build upon this work non-commercially, and license their derivative works on different terms, provided the original work is properly cited, appropriate credit is given, any changes made indicated, and the use is non-commercial. See: <http://creativecommons.org/licenses/by-nc/4.0/>.

### ORCID iDs

Jie Zhang <http://orcid.org/0000-0002-1397-5224>

Min Wu <http://orcid.org/0009-0005-7952-5997>

Xiangming Ye <http://orcid.org/0000-0003-2230-6329>

Benyan Luo <http://orcid.org/0000-0002-9892-5778>

Li Zhang <http://orcid.org/0000-0002-8966-7594>

## REFERENCES

- Sacco S, Marini C, Totaro R, *et al*. A population-based study of the incidence and prognosis of lacunar stroke. *Neurology (Ecricon)* 2006;66:1335–8.
- Regenhardt RW, Das AS, Lo EH, *et al*. Advances in Understanding the Pathophysiology of Lacunar Stroke: A Review. *JAMA Neurol* 2018;75:1273–81.
- Bezerra DC, Sharrett AR, Matsushita K, *et al*. Risk factors for lacune subtypes in the Atherosclerosis Risk in Communities (ARIC) Study. *Neurology (Ecricon)* 2012;78:102–8.
- Traylor M, Persyn E, Tomppo L, *et al*. Genetic basis of lacunar stroke: a pooled analysis of individual patient data and genome-wide association studies. *Lancet Neurol* 2021;20:351–61.
- Traylor M, Bevan S, Baron J-C, *et al*. Genetic Architecture of Lacunar Stroke. *Stroke* 2015;46:2407–12.
- Duering M, Csanadi E, Gesierich B, *et al*. Incident lacunes preferentially localize to the edge of white matter hyperintensities: insights into the pathophysiology of cerebral small vessel disease. *Brain (Bacau)* 2013;136:2717–26.
- Persyn E, Hanscombe KB, Howson JMM, *et al*. Genome-wide association study of MRI markers of cerebral small vessel disease in 42,310 participants. *Nat Commun* 2020;11:2175.
- Zhang H, Schneider T, Wheeler-Kingshott CA, *et al*. NODDI: practical in vivo neurite orientation dispersion and density imaging of the human brain. *Neuroimage* 2012;61:1000–16.
- Sabisz A, Naumczyk P, Marcinkowska A, *et al*. Aging and Hypertension - Independent or Intertwined White Matter Impairing Factors? Insights From the Quantitative Diffusion Tensor Imaging. *Front Aging Neurosci* 2019;11:35.
- Hainsworth AH, Markus HS, Schneider JA. Cerebral Small Vessel Disease, Hypertension, and Vascular Contributions to Cognitive Impairment and Dementia. *Hypertension* 2024;81:75–86.
- de Havenon A, Majersik JJ, Tirschwell DL, *et al*. Blood pressure, glyemic control, and white matter hyperintensity progression in type 2 diabetics. *Neurology (Ecricon)* 2019;92:e1168–75.
- Taylor-Bateman V, Gill D, Georgakis MK, *et al*. Cardiovascular Risk Factors and MRI Markers of Cerebral Small Vessel Disease: A Mendelian Randomization Study. *Neurology (Ecricon)* 2022;98:e343–51.
- Rutten-Jacobs LCA, Tozer DJ, Duering M, *et al*. Genetic Study of White Matter Integrity in UK Biobank (N=8448) and the Overlap With Stroke, Depression, and Dementia. *Stroke* 2018;49:1340–7.
- Prins ND, Scheitens P. White matter hyperintensities, cognitive impairment and dementia: an update. *Nat Rev Neurol* 2015;11:157–65.
- Wardlaw JM, Benveniste H, Nedergaard M, *et al*. Perivascular spaces in the brain: anatomy, physiology and pathology. *Nat Rev Neurol* 2020;16:137–53.
- Kurki MI, Karjalainen J, Palta P, *et al*. Data from: FinnGen summary statistics release 10. 2024. Available: <https://finngen.gitbook.io/documentation/v/r10/data-download>

- 17 Mahajan A, Taliun D, Thurner M, *et al.* Data from: Type 2 diabetes GWAS summary statistics. *GWAS Catalog* 2024. Available: <https://www.ebi.ac.uk/gwas/studies/GCST002087>
- 18 Meurs JB, Pare G, Schwartz SM, *et al.* Data from: Plasma homocysteine concentrations GWAS summary statistics. *Am J Clin Nutr* 2024. Available: <https://doi.org/10.1038/s41588-018-0241-6>
- 19 Liu M, Jiang Y, Wedow R, *et al.* Data from: Cigarettes per day GWAS summary statistics. *GSCAN Consortium* 2024.
- 20 Codd V, Wang Q, Allara E, *et al.* Data from: Leukocyte telomere length GWAS summary statistics. *MRC-IEU OpenGWAS* 2025. Available: <https://gwas.mrcieu.ac.uk/datasets/ieu-b-4879>
- 21 McCartney DL, Min JL, Richmond RC, *et al.* Data from: Intrinsic epigenetic age acceleration GWAS. *GWAS Catalog* 2025. Available: <https://www.ebi.ac.uk/gwas/studies/GCST90014290>
- 22 Traylor M, Persyn E, Tomppo L, *et al.* Data from: Lacunar stroke GWAS summary statistics. *MRC-IEU OpenGWAS* 2024. Available: <https://gwas.mrcieu.ac.uk/datasets/ebi-a-GCST90014123>
- 23 Adams HP Jr, Bendixen BH, Kappelle LJ, *et al.* Classification of subtype of acute ischemic stroke. Definitions for use in a multicenter clinical trial. TOAST. Trial of Org 10172 in Acute Stroke Treatment. *Stroke* 1993;24:35–41.
- 24 Rajajee V, Kidwell C, Starkman S, *et al.* Diagnosis of lacunar infarcts within 6 hours of onset by clinical and CT criteria versus MRI. *J Neuroimaging* 2008;18:66–72.
- 25 Smith SM, Douaud G, Chen W, *et al.* Data from: UK Biobank brain imaging GWAS summary statistics (imaging-derived phenotypes for white matter microstructure, white matter hyperintensities and brain volumes). *GWAS Catalog* 2024. Available: <https://www.ebi.ac.uk/gwas/publications/33875891>
- 26 Duperron MG, Knol MJ, Le Grand Q, *et al.* Data from: Perivascular space burden GWAS summary statistics. *Nat Med* 2024. Available: <https://doi.org/10.1038/s41591-023-02268-w>
- 27 Said S, Pazoki R, Karhunen V, *et al.* Data from: C-reactive protein GWAS summary statistics. *GWAS Catalog* 2025. Available: <https://www.ebi.ac.uk/gwas/studies/ebi-a-GCST90029070>
- 28 Konieczny MJ, Omarov M, Zhang L, *et al.* Data from: Vascular endothelial growth factor A GWAS summary statistics. *GWAS Catalog* 2025. Available: <https://www.ebi.ac.uk/gwas/studies/GCST90428438>
- 29 Burgess S, Davies NM, Thompson SG. Bias due to participant overlap in two-sample Mendelian randomization. *Genet Epidemiol* 2016;40:597–608.
- 30 Burgess S, Daniel RM, Butterworth AS, *et al.* Network Mendelian randomization: using genetic variants as instrumental variables to investigate mediation in causal pathways. *Int J Epidemiol* 2015;44:484–95.
- 31 Zhang J. R code for: Mendelian randomisation analyses of risk factors, white matter microstructure, and lacunar stroke. *GitHub* 2024. Available: [https://github.com/jzhang-neuro/MR\\_WM\\_LS](https://github.com/jzhang-neuro/MR_WM_LS)
- 32 Alber J, Alladi S, Bae H-J, *et al.* White matter hyperintensities in vascular contributions to cognitive impairment and dementia (VCID): Knowledge gaps and opportunities. *Alzheimers Dement (N Y)* 2019;5:107–17.
- 33 Jorgensen DR, Shaaban CE, Wiley CA, *et al.* A population neuroscience approach to the study of cerebral small vessel disease in midlife and late life: an invited review. *Am J Physiol Heart Circ Physiol* 2018;314:H1117–36.
- 34 Wardlaw JM, Valdés Hernández MC, Muñoz-Maniega S. What are white matter hyperintensities made of? Relevance to vascular cognitive impairment. *J Am Heart Assoc* 2015;4:e001140.
- 35 Dozono K, Ishii N, Nishihara Y, *et al.* An autopsy study of the incidence of lacunes in relation to age, hypertension, and arteriosclerosis. *Stroke* 1991;22:993–6.
- 36 Topakian R, Barrick TR, Howe FA, *et al.* Blood-brain barrier permeability is increased in normal-appearing white matter in patients with lacunar stroke and leucoaraiosis. *J Neurol Neurosurg Psychiatry* 2010;81:192–7.
- 37 Tarumi T, Thomas BP, Wang C, *et al.* Ambulatory pulse pressure, brain neuronal fiber integrity, and cerebral blood flow in older adults. *J Cereb Blood Flow Metab* 2019;39:926–36.
- 38 Takeuchi H, Kawashima R. Effects of Diastolic Blood Pressure on Brain Structures and Cognitive Functions in Middle and Old Ages: Longitudinal Analyses. *Nutrients* 2022;14:2464.
- 39 Low A, Mak E, Stefaniak JD, *et al.* Peak Width of Skeletonized Mean Diffusivity as a Marker of Diffuse Cerebrovascular Damage. *Front Neurosci* 2020;14:238.
- 40 Reijmer YD, Freeze WM, Leemans A, *et al.* The effect of lacunar infarcts on white matter tract integrity. *Stroke* 2013;44:2019–21.
- 41 Alexander AL, Lee JE, Lazar M, *et al.* Diffusion tensor imaging of the brain. *Neurotherapeutics* 2007;4:316–29.
- 42 Wartolowska KA, Webb AJS. Blood Pressure Determinants of Cerebral White Matter Hyperintensities and Microstructural Injury: UK Biobank Cohort Study. *Hypertension* 2021;78:532–9.
- 43 Mouchtouris N, Ailes I, Gooch R, *et al.* Quantifying blood-brain barrier permeability in patients with ischemic stroke using non-contrast MRI. *Magn Reson Imaging* 2024;109:165–72.
- 44 Salat DH, Williams VJ, Leritz EC, *et al.* Inter-individual variation in blood pressure is associated with regional white matter integrity in generally healthy older adults. *Neuroimage* 2012;59:181–92.
- 45 Yu K, Chen X-F, Guo J, *et al.* Assessment of bidirectional relationships between brain imaging-derived phenotypes and stroke: a Mendelian randomization study. *BMC Med* 2023;21:271.
- 46 Coenen VA, Schlaepfer TE, Sajonz B, *et al.* Tractographic description of major subcortical projection pathways passing the anterior limb of the internal capsule. Corticopetal organization of networks relevant for psychiatric disorders. *Neuroimage Clin* 2020;25:102165.
- 47 Feekes JA, Hsu S-W, Chaloupka JC, *et al.* Tertiary microvascular territories define lacunar infarcts in the basal ganglia. *Ann Neurol* 2005;58:18–30.
- 48 Caplan LR. Intracranial branch atheromatous disease: a neglected, understudied, and underused concept. *Neurology (Ecricon)* 1989;39:1246–50.
- 49 Fisher CM. The arterial lesions underlying lacunes. *Acta Neuropathol* 1968;12:1–15.
- 50 Lammie GA, Brannan F, Slattery J, *et al.* Nonhypertensive cerebral small-vessel disease. An autopsy study. *Stroke* 1997;28:2222–9.
- 51 Mishra A, Malik R, Hachiya T, *et al.* Stroke genetics informs drug discovery and risk prediction across ancestries. *Nature New Biol* 2022;611:115–23.
- 52 Ueshima H, Sekikawa A, Miura K, *et al.* Cardiovascular disease and risk factors in Asia: a selected review. *Circulation* 2008;118:2702–9.